Monthly Notices of the ROYAL ASTRONOMICAL SOCIETY

MNRAS **509,** 5231–5236 (2022)
Advance Access publication 2021 November 2

https://doi.org/10.1093/mnras/stab3175

Where have all the interstellar silicon carbides gone?

Tao Chen [1,2]† C. Y. Xiao,[1★]† Aigen Li[3★] and C. T. Zhou[4★]

[1]*Department of Astronomy, Beijing Normal University, Beijing 100875, China*
[2]*Department of Theoretical Chemistry and Biology, Royal Institute of Technology, SE-10691 Stockholm, Sweden*
[3]*Department of Physics and Astronomy, University of Missouri, Columbia, MO 65211, USA*
[4]*College of Engineering Physics, Shenzhen Technology University, Shenzhen 518118, China*

Accepted 2021 October 28. Received 2021 October 13; in original form 2021 July 22

ABSTRACT

The detection of the 11.3 μm emission feature characteristic of the Si–C stretch in carbon-rich evolved stars reveals that silicon carbide (SiC) dust grains are condensed in the outflows of carbon stars. SiC dust could be a significant constituent of interstellar dust since it is generally believed that carbon stars inject a considerable amount of dust into the interstellar medium (ISM). The presence of SiC dust in the ISM is also supported by the identification of pre-solar SiC grains of stellar origin in primitive meteorites. However, the 11.3 μm absorption feature of SiC has never been seen in the ISM, and oxidative destruction of SiC is often invoked. In this work, we quantitatively explore the destruction of interstellar SiC dust through oxidation based on molecular dynamics simulations and density functional theory calculations. We find that the reaction of an oxygen atom with SiC molecules and clusters is exothermic and could cause CO-loss. Nevertheless, even if this is extrapolable to bulk SiC dust, the destruction rate of SiC dust through oxidation could still be considerably smaller than the (currently believed) injection rate from carbon stars. Therefore, the lack of the 11.3 μm absorption feature of SiC dust in the ISM remains a mystery. A possible solution may lie in the currently believed stellar injection rate of SiC (which may have been overestimated) and/or the size of SiC dust (which may actually be considerably smaller than submicron in size).

Key words: stars: AGB and post-AGB – stars: carbon – circumstellar matter – stars: mass-loss – dust, extinction – ISM: lines and bands.

1 INTRODUCTION

Nearly nine decades ago, Wildt (1933) had already argued that solid silicon carbide (SiC) grains might form in N-type stars. It is now well recognized that SiC solids are a major dust species, second to amorphous carbon grains, condensed in the cool atmospheres of mass-losing, carbon-rich asymptotic giant branch (AGB) stars (e.g. see Nanni et al. 2021). This was originally computationally demonstrated over half a century ago by Friedemann (1969) and Gilman (1969) based on molecular equilibrium calculations, and observationally confirmed later by Treffers & Cohen (1974), who, for the first time, detected in two carbon stars, IRC+10216 and IRC+30219, a broad emission band in between 788 and 973 cm^{-1} attributed to SiC dust. Subsequent spectroscopic observations have revealed the widespread presence of SiC grains in carbon stars through the prominent 11.3 μm emission feature characteristic of the Si–C stretch of SiC solids (Speck, Barlow & Skinner 1997; Mutschke et al. 1999).[1] In addition, pre-solar SiC grains of stellar origin have also been identified in primitive meteorites based on isotope anomalies (e.g. see Bernatowicz et al. 1987).

Although the exact mass fraction of the condensates in carbon stars, which are in the form of SiC, is not precisely known and it depends on stellar mass and metallicity (Nanni et al. 2021), radiative transfer modelling of the observed infrared emission of carbon stars has shown that the mass ratio of SiC to amorphous carbon could be as much as ∼25 per cent for the Milky Way (e.g. see Groenewegen et al. 1998), ∼43 per cent for the Large Magellanic Cloud, and ∼11 per cent for the Small Magellanic Cloud (Groenewegen et al. 2009; Nanni et al. 2019). Theoretical dust-yield calculations have predicted that the mass fraction of SiC over the total dust (i.e. SiC plus amorphous carbon) produced in carbon stars of an initial mass of 3 $M_\odot$ around solar metallicity is ∼25 per cent (Nanni et al. 2013; also see Zhukovska & Henning 2013), although different AGB models produce different yields at varying metallicity because of the uncertainties in modelling the mass-loss and third dredge-up processes (e.g. see Ventura et al. 2012, 2014, 2018; Nanni et al. 2013, 2014, 2019).

Solid grains – SiC and amorphous carbon condensed in carbon stars as well as silicates and oxides condensed in oxygen-rich stars – will be driven out of the stellar atmospheres and injected into the

★ E-mail: xiaocunying@bnu.edu.cn (CYX); LiA@missouri.edu (AL); zcangtao@sztu.edu.cn (CTZ)
† TC and CYX contributed equally.
[1]In principle, essentially all carbon star should make SiC. Observationally, SiC dust is harder to detect in redder stars as the contrast with amorphous carbon becomes smaller. The 11.3 μm SiC feature strength with respect to the dust thermal emission continuum has been seen to increase with the stellar metallicity and show a trend with the stellar mass-loss rate (e.g. see Sloan et al. 2016; Kraemer et al. 2019; Nanni et al. 2021).

© 2021 The Author(s)
Published by Oxford University Press on behalf of Royal Astronomical Society

Downloaded from https://academic.oup.com/mnras/article/509/4/5231/6415899 by University of Missouri-Columbia user on 13 December 2021

interstellar medium (ISM) by radiation pressure (see Dorfi & Höfner 1991). If the contribution of carbon stars to the Galactic dust budget is about comparable to that of oxygen-rich stars as generally believed (e.g. see Gehrz 1989), then SiC should be a significant constituent of interstellar dust. However, the non-detection of the characteristic 11.3 μm feature of SiC in the ISM puts this at odds (Whittet, Duley & Martin 1990; Chiar & Tielens 2006; Min et al. 2007). In this work, we explore the physical and chemical processes subjected by SiC in the ISM, with special attention paid to the destruction of SiC by oxidation. We apply the Born–Oppenheimer molecular dynamics (BOMD; Helgaker, Uggerud & Jensen 1990; Uggerud & Helgaker 1992) and density functional theory (DFT; Lee, Yang & Parr 1988; Becke 1992) to investigate the oxidation reaction pathway related to SiC grains in the ISM. The DFT technique is among the most popular and versatile methods for computational quantum mechanical modelling of molecules and clusters. In comparison with other quantum chemical methods, DFT simplifies the *N*-body problem to a tractable 3*N* non-interacting system, which makes DFT more efficient and scalable for large systems. In BOMD simulations, the energies and forces are computed from DFT at quantum levels. Therefore, the BOMD method is more accurate than classical molecular dynamics in which the energies and forces are calculated from empirical formulae or force fields.

2 COMPUTATIONAL METHODS

A typical, submicron-sized SiC grain contains hundreds of millions of atoms (e.g. there are $\sim 4 \times 10^8$ atoms in a spherical SiC grain of radius $a = 0.1$ μm). Even for SiC nanoparticles, it is extremely expensive to study such systems with *ab initio* methods like BOMD and DFT, requiring tremendous computational power and time. Nevertheless, it is generally believed that SiC grains are built up via bottom-up processes, starting with small gas-phase molecules and successive growth to clusters by molecular additions. Thus, SiC clusters are indispensable for the formation of SiC grains – they are the initial states of SiC grains (e.g. see Gobrecht et al. 2017). Therefore, SiC molecules and clusters could be reasonable candidates or alternatives of SiC grains for molecular dynamics modelling. To this end, we consider the most favourable structures of Si_3C_3 and $Si_{12}C_{12}$,[2] with the former representing a triangle structure (see fig. 4a of Gobrecht et al. 2017, also see Mühlhäuser et al. 1993) with a high surface-to-volume ratio and the latter exhibiting a spherical structure (see fig. 16a of Gobrecht et al. 2017, also see Watkins et al. 2009) and possessing a low surface-to-volume ratio. Si_3C_3 is selected because it is the smallest cluster with a 3D structure (see Gobrecht et al. 2017) and thus allows us to investigate the reactions for the low-end cluster. $Si_{12}C_{12}$ is selected because of its bucky-like symmetrical structure, which minimizes the considerations of the incident directions of oxygen atoms. $Si_{16}C_{16}$ is also symmetrical in structure, but it is computationally more expensive (see Gobrecht et al. 2017).

To evaluate the stability or reactivity of the studied molecule or cluster, we calculate the binding and dissociation energies and transition barriers for each target system, using DFT as implemented in the GAUSSIAN16 package (Frisch et al. 2016). All structures are optimized to their ground states using the 6-311++G(2d,p) basis set. Here, the Slater-type atomic orbitals are described by 'basis functions', and each basis function is described by a sum of several Gaussian functions. To take the intermolecular forces into account, the D3 version of Grimme's dispersion with Becke–Johnson damping (Grimme, Ehrlich & Goerigk 2011) is included in the calculations. Here, 'D3' denotes a function of interatomic distances, which contains adjustable parameters that are fitted to the conformational and interaction energies computed using high-level methods.

The vibrational frequencies are calculated under the harmonic oscillator approximation for the optimized geometries. The transition states are estimated based on our molecular dynamics simulations, followed by relaxed scanning (with geometry optimization at each point) on the potential energy surface. The transition barrier is calculated as the energy difference between the ground states of the reactant and the transition state. For reactions without transition state, the dissociation energy is computed as the energy difference between the ground states of the reactant and the product. The intermolecular forces are taken into account in all the calculations. The dynamical processes are simulated using BOMD (Helgaker et al. 1990; Uggerud & Helgaker 1992) as implemented in the GAUSSIAN16 package (Frisch et al. 2016). The B3LYP hybrid functional in combination with the 6-31G(d,p) basis set is utilized for the BOMD simulations. For all these simulations, again, the D3 version of Grimme's dispersion with Becke–Johnson damping (Grimme et al. 2011) is also included.

3 RESULTS

Over 30 years ago, Whittet et al. (1990) searched for the 11.3 μm absorption band of SiC in the diffuse ISM along the line of sight towards the Galactic Centre. The lack of any spectral evidence for solid SiC led Whittet et al. (1990) to place an upper limit on the abundance of silicon relative to hydrogen (i.e. Si/H) in SiC dust to be at most ∼5 per cent of that in silicate dust. Similarly, based on the nondetection of the SiC 11.3 μm absorption feature along the lines of sight toward WR 98a and WR 112, two heavily obscured Galactic WC-type Wolf-Rayet stars, Chiar & Tielens (2006) obtained an upper limit of ∼4 per cent on the fraction of Si atoms that are incorporated into SiC. Min et al. (2007) estimated the mass fraction of interstellar SiC dust to be ∼3 per cent of interstellar silicate dust (of composition $Mg/(Mg + Fe) > 0.9$ and $O/Si \approx 3.5$), corresponding to ∼8 per cent of the Si atoms available inthe ISM. Whittet et al. (1990) speculated that SiC grains could be destroyed in the ISM by oxidation. Motivated by this, we first model the interaction between a Si_3C_3 molecule and an incident oxygen atom. This applies to the diffuse ISM where atomic oxygen is the dominant form of gaseous oxygen. The oxidation of SiC solids by O_2 has been extensively studied experimentally (e.g. see Ervin 1958) and is not relevant since there is little O_2 in the ISM (e.g. see Larsson et al. 2007). In dense molecular clouds where oxygen is mostly locked up in water ice, SiC dust, if present, is expected to be coated by a layer of water ice and oxidation is unlikely since the reaction of SiC with water to produce SiO_2 and methane only takes place at a temperature of above 1300°C (e.g. see Park et al. 2014).

As the oxygen atom is much smaller than a SiC cluster or grain, the incident oxygen atom would only influence a few atoms in the target SiC cluster or grain, i.e. the reaction would only take place in an area near the incident atom and depends on the incident direction. Fig. 1 shows the BOMD simulations for collisions between a Si_3C_3 molecule and an incident oxygen atom arriving from three different directions. The simulations demonstrate that, due to the impact of an oxygen atom, CO and SiO molecules can be released rapidly from

[2] Si_3C_3 has many isomers, and the number of structural isomers for $Si_{12}C_{12}$ gets literally astronomical. Here, we are confined to the isomers with the lowest energy.

Downloaded from https://academic.oup.com/mnras/article/509/4/5231/6415899 by University of Missouri-Columbia user on 13 December 2021

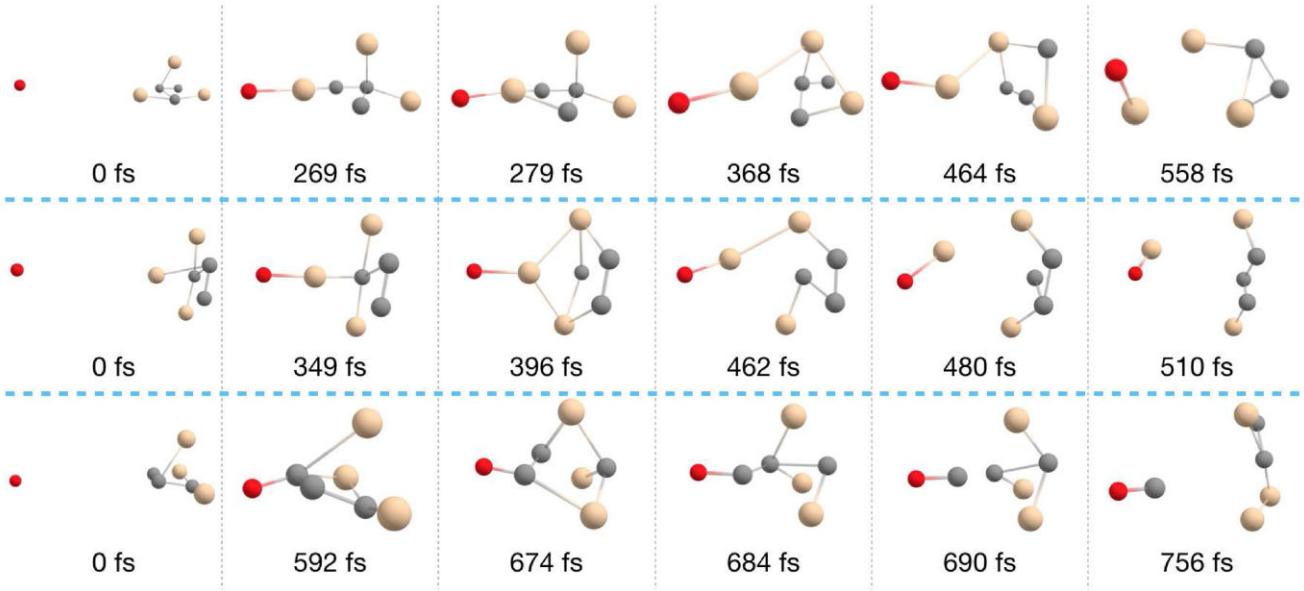

Figure 1. Snapshots from molecular dynamics simulations for collisions between an oxygen atom (red ball) and a Si_3C_3 molecule (in which grey balls represent carbon atoms and yellow balls correspond to silicon atoms), with the oxygen atom arriving from three different directions. The actual time in the simulation is shown beneath each molecular structure. SiO-loss (upper and middle panels) and CO-loss (bottom panel) can be seen on the rightmost panels.

the molecule within 1 ps. The fragmentation products are highly dependent on the incoming direction of the oxygen atom: If the oxygen atom first collides with a carbon atom, then a CO molecule is formed and ejected, while a SiO-loss would be triggered if the incident oxygen atom first hits a silicon atom.

To better understand the reaction mechanism, DFT calculations for the three reaction scenarios, as illustrated in Fig. 1, are performed and shown in Fig. 2. The corresponding binding energies for $O + Si_3C_3$ and dissociation energies for Si_3C_3O–CO or Si_3C_3O–SiO are illustrated in Fig. 2 as well. Most prominently, the reactions for absorbing an oxygen atom to a Si_3C_3 molecule are *exothermic*, which release $\sim$7–9 eV energy, depending on the incoming direction of the incident oxygen atom. This is not surprising since association reactions of the form $A + B \rightarrow AB$ are usually exothermic, as the number of bonds is increased in the product. The energy generated from these reactions will traverse through all of the vibrational modes of the molecule, and the chemical bonds with lower binding energies will be dissociated. Moreover, for the Si_3C_3O system, SiO-loss is also an exothermic reaction, which releases $\sim$ 1 eV energy. In contrast, CO has a binding energy of $\sim$ 0.6 eV, and therefore it requires $\sim$ 0.6 eV to eject CO from the Si_3C_3O system. However, with the much larger amount of energy ($\sim$7–9 eV) gained from the first step, such a low binding energy can be easily crossed, leading to a rapid CO-loss.

The collisions between an oxygen atom with larger molecules, e.g. $Si_{12}C_{12}$, demonstrate a rather different scenario. Fig. 3 shows the BOMD simulations for collisions between an oxygen atom and a $Si_{12}C_{12}$ molecule. No fragmentation is found; instead, the oxygen atom is captured by the $Si_{12}C_{12}$ molecule. The symmetry of the molecule is broken due to the incoming oxygen atom, which forms two new covalent bonds, one connected with a carbon atom and the other one connected with a silicon atom. The DFT calculations show that, as illustrated in Fig. 4, the absorption of an oxygen atom is still an exothermic reaction, which releases $\sim$ 7.5 eV energy. However, the dissociation of CO and SiO requires $\sim$ 2.6 and $\sim$ 4.0 eV, respectively. Due to its larger size, $Si_{12}C_{12}$ could redistribute the excess energy across its degrees of freedom to avoid fragmentation.

Nevertheless, in the diffuse ISM, oxygen atoms are far more abundant than SiC grains.[3] It is therefore highly probable that a SiC grain would be hit by multiple oxygen atoms. Fig. 5 shows the collisions of $Si_{12}C_{12}O$ with another oxygen atom. The $Si_{12}C_{12}O$ molecule is adopted from the simulation illustrated in Fig. 3 but is set to its vibrationally ground state. Two opposite incident directions are simulated for the incoming oxygen atom. In both cases, we see CO-loss within 1 ps. This is because the presence of oxygen atoms (aka O-substituted molecules) decreases the transition energy barriers in the region where the oxygen atom is located, which makes CO-losses highly favourable in comparison to other channels.

4 DISCUSSION

We have shown in Section 3 that the reaction between an oxygen atom and a SiC molecule is exothermic and would result in CO-loss almost instantly for small SiC molecules, or after the absorption of one or several oxygen atoms for large SiC molecules. Therefore, the destruction rate of SiC in the ISM is essentially determined by the collision rate of oxygen atoms with SiC grains. Let n_O be the number density of oxygen atoms in the diffuse ISM, v_O be the mean thermal velocity of oxygen atoms, and τ_{coll} be the collision time-scale of an oxygen atom with a SiC grain of radius a. The collision rate (in s^{-1}) is $\tau_{coll}^{-1} = n_O\, v_O\, \pi a^2$, where $n_O \approx [O/H]_{gas} n_H$, $v_O = \sqrt{3k_B T_{gas}/m_O}$, n_H is the hydrogen number density, k_B is the Boltzmann constant, T_{gas} is the gas temperature, and m_O is the mass of an oxygen atom. If we adopt an interstellar gas-phase oxygen abundance of $[O/H]_{gas} =$

[3]If we take a gas-phase abundance of $[O/H]_{gas} = 320$ ppm for atomic oxygen in the diffuse ISM (Meyer, Jura & Cardelli 1998), and assume that all SiC grains have the same size of $a = 0.1$ μm and consume an upper limit of 5 ppm of Si/H (Whittet et al. 1990), the number density of oxygen atoms exceeds that of SiC grains by a factor of $\sim 1.3 \times 10^{10}$.

Downloaded from https://academic.oup.com/mnras/article/509/4/5231/6415899 by University of Missouri-Columbia user on 13 December 2021

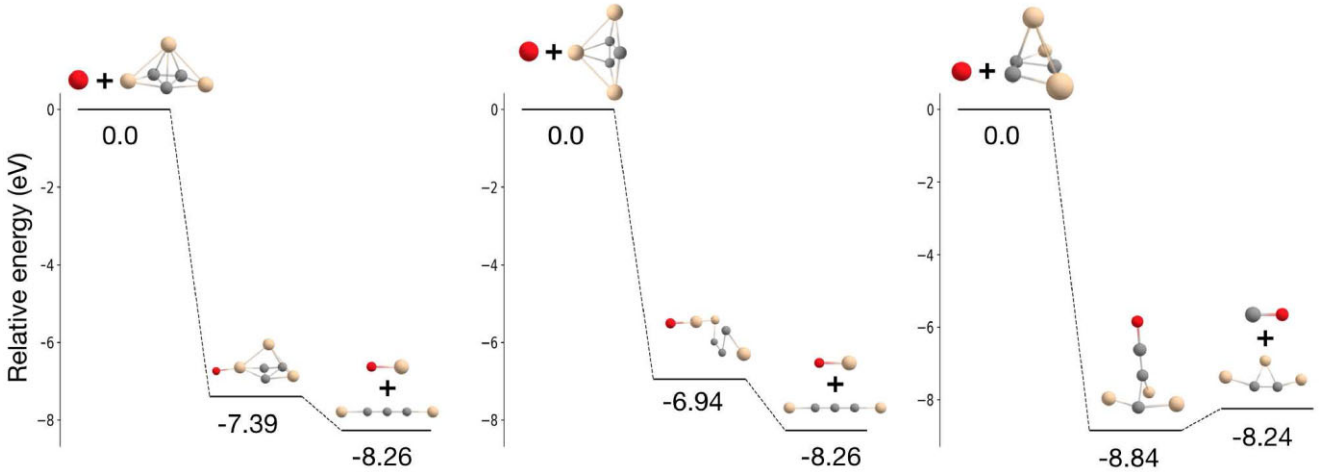

Figure 2. Calculated binding and dissociation energies for reactions between a Si_3C_3 molecule and an incident oxygen atom arriving at three different positions.

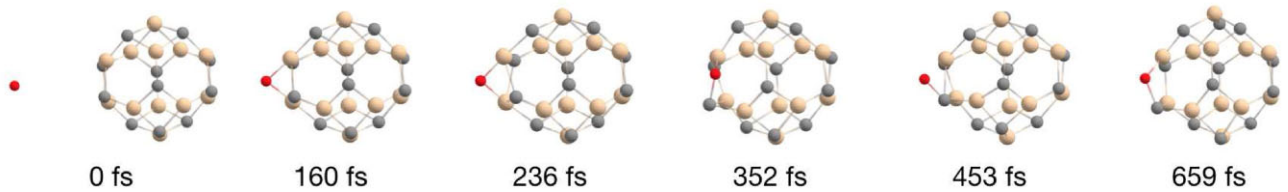

Figure 3. Snapshots from molecular dynamics simulations for collisions between an oxygen atom (red ball) and a $Si_{12}C_{12}$ molecule. Due to the high symmetry of $Si_{12}C_{12}$, only one incident direction is simulated for the oxygen atom.

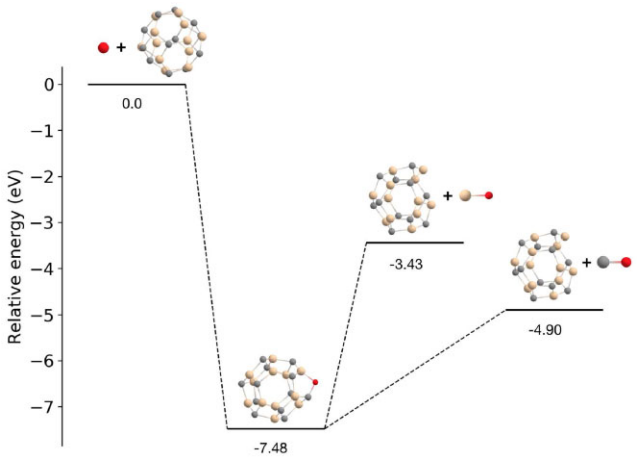

Figure 4. Calculated binding and dissociation energies for reactions between a $Si_{12}C_{12}$ molecule and an incident oxygen atom.

320 ppm (Meyer et al. 1998), $n_{\rm H} = 1\,{\rm cm}^{-3}$, and $T_{\rm gas} = 100\,{\rm K}$ for the diffuse ISM, we obtain $\tau_{\rm coll} \approx 2.52 \times 10^8 \times (0.1\,\mu{\rm m}/a)^2\,{\rm s} \approx 7.99 \times (0.1\,\mu{\rm m}/a)^2$ yr.

Let $[{\rm Si/H}]_{\rm SiC}$ be the abundance of silicon (relative to hydrogen) tied up in SiC dust in the ISM, $\mu_{\rm SiC} = 40$ be the molecular weight of SiC, $\rho_{\rm SiC} \approx 3.2\,{\rm g\,cm}^{-3}$ be the mass density of SiC dust,[4] $m_{\rm SiC} = (4/3)\pi a^3 \rho_{\rm SiC}$ be the mass of a spherical SiC grain of radius a, and $M_{\rm H}$ be the total interstellar hydrogen gas mass in the Milky Way. The total number of SiC grains would be $N_{\rm SiC} \approx M_{\rm H}\,[{\rm Si/H}]_{\rm SiC}\,\mu_{\rm SiC}/m_{\rm SiC} \lesssim 1.44 \times 10^{53}\,(0.1\,\mu{\rm m}/a)^3$, if we adopt $M_{\rm H} = 4.9 \times 10^9\,{\rm M}_\odot$ (Draine 2011), $[{\rm Si/H}]_{\rm SiC} \lesssim 5$ ppm (Whittet et al. 1990), and assume that all SiC grains have the same size a. If each collision of an oxygen atom with a SiC grain results in an ejection of CO, we would expect a total SiC dust mass destruction rate of $({\rm d}M/{\rm d}t)^{\rm des}_{\rm SiC} \approx 12 m_{\rm H} N_{\rm SiC}/\tau_{\rm coll} \lesssim 1.80 \times 10^{-4}\,(0.1\,\mu{\rm m}/a)\,{\rm M}_\odot\,{\rm yr}^{-1}$.

The injection rate of carbon dust from all carbon-rich objects including C, R, N, and S stars into the ISM was estimated to be $({\rm d}M/{\rm d}t)^{\rm pro}_{\rm C} \approx 0.003$–$0.01\,{\rm M}_\odot\,{\rm yr}^{-1}$ (Gehrz 1989). Let us assume the SiC dust injection rate from evolved stars to be 10 per cent of that of carbon dust (see Groenewegen et al. 1998, 2009; Nanni et al. 2013, 2019). We would then expect that each year carbon stars eject about $(3$–$10) \times 10^{-4}\,{\rm M}_\odot$ of SiC dust into the ISM, i.e. $({\rm d}M/{\rm d}t)^{\rm pro}_{\rm SiC} \approx 10$ per cent $\times\,({\rm d}M/{\rm d}t)^{\rm pro}_{\rm C} \approx (3$–$10) \times 10^{-4}\,{\rm M}_\odot\,{\rm yr}^{-1}$. Compared with the SiC destruction rate of $({\rm d}M/{\rm d}t)^{\rm des}_{\rm SiC} \lesssim 1.80 \times 10^{-4}\,(0.1\,\mu{\rm m}/a)\,{\rm M}_\odot\,{\rm yr}^{-1}$, it is clear that one requires the interstellar SiC grains to be smaller than $\sim 0.02\,\mu$m [for $({\rm d}M/{\rm d}t)^{\rm pro}_{\rm SiC} = 3 \times 10^{-4}\,{\rm M}_\odot\,{\rm yr}^{-1}$] or $\sim 0.06\,\mu$m [for $({\rm d}M/{\rm d}t)^{\rm pro}_{\rm SiC} = 1 \times 10^{-3}\,{\rm M}_\odot\,{\rm yr}^{-1}$] in order for the destruction rate to exceed the current injection rate from carbon stars, i.e. $({\rm d}M/{\rm d}t)^{\rm des}_{\rm SiC} \gtrsim ({\rm d}M/{\rm d}t)^{\rm pro}_{\rm SiC}$. However, pre-solar SiC grains of stellar origin identified in primitive meteorites are mostly submicron-sized.[5]

[4]We note that such a mass density is applicable for bulk, macroscopic SiC dust. For small SiC clusters, this would underestimate the actual 'size' since small SiC clusters are hollow and not compactly packed (e.g. such a mass density would imply a radius of $a \approx 3.90$ Å for a spherical $Si_{12}C_{12}$ cluster).

[5]While Amari et al. (1994) found that ~20 per cent of all the pre-solar SiC grains seen in the Murchison meteorite are in the fractions greater than 1 μm and only about 4 per cent in the fraction less than 0.3 μm, NanoSIMS (nanoscale secondary ion mass spectrometry) measurements of the Murchison

Downloaded from https://academic.oup.com/mnras/article/509/4/5231/6415899 by University of Missouri-Columbia user on 13 December 2021

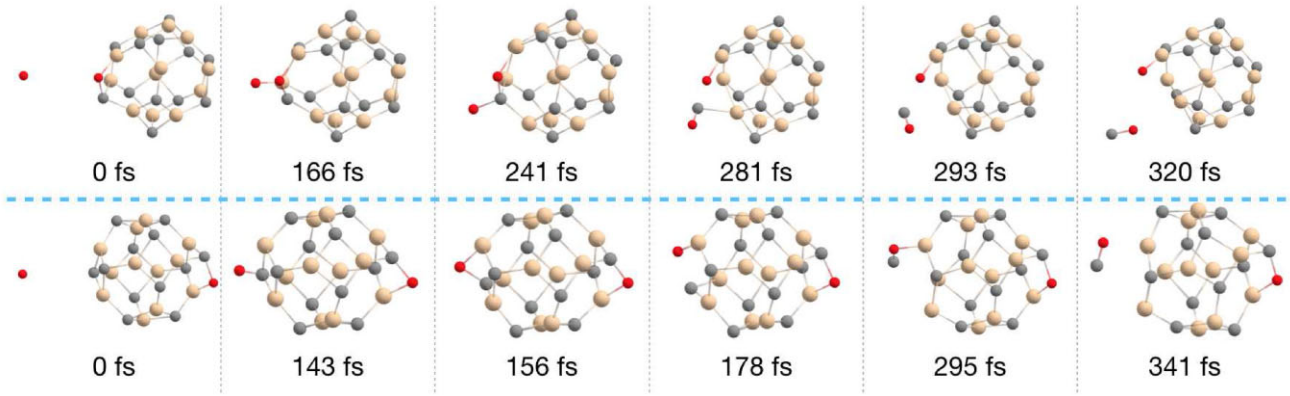

Figure 5. Snapshots from molecular dynamics simulations for collisions between an oxygen atom (red ball) and a $Si_{12}C_{12}O$ molecule from two opposite directions.

As we have already generously assumed that one collision leads to the ejection of one CO molecule despite that for large SiC molecules multiple collisions are needed, we conclude that the destruction rate of SiC dust by oxidation is unlikely larger than the stellar injection rate and therefore the non-detection of the 11.3 μm absorption feature of SiC dust in the diffuse ISM cannot be explained by the destruction of SiC dust through oxidation. It is true that the kinetic reactions of oxygen atoms with bulk, macroscopic SiC dust certainly differ from that of oxygen atoms with molecular SiC clusters. However, the destruction rates of SiC dust derived above do not rely on the exact oxidation rates of SiC clusters. Indeed, the only assumption made in deriving $(\mathrm{d}M/\mathrm{d}t)_{\mathrm{SiC}}^{\mathrm{des}}$ is that each collision of an oxygen atom with a SiC dust grain would result in an ejection of CO. As mentioned above, this would result in an overestimation of $(\mathrm{d}M/\mathrm{d}t)_{\mathrm{SiC}}^{\mathrm{des}}$ since for large SiC clusters a single collision is unlikely capable of releasing CO. It is worth noting that Draine (1979) explored the chemisputtering of graphite in the ISM with abundant H and O atoms and found that graphite does not react with these species at low temperatures.

While the 11.3 μm absorption feature could be suppressed in large SiC grains of $a > 1$ μm, pre-solar SiC grains, as mentioned earlier, have indicated the predominant presence of submicron-sized SiC grains. Perhaps submicron-sized SiC grains only constitute a small fraction of the SiC dust condensed in carbon stars and then ejected into the ISM. Cristallo et al. (2020) examined the evolution of the AGB stars that polluted the Solar system around 4.57 Gyr ago and found that the submicron-sized pre-solar SiC grains predominantly originated from AGB stars with solar metallicity and an initial mass of $\sim 2\,\mathrm{M}_{\odot}$. Theoretical calculations have shown that the typical grain size of SiC condensed in AGB stars can be dependent on the stellar metallicity and can be smaller than pre-solar SiC grains for stars with metallicities lower than solar (e.g. see figs 11 and 12 in Nanni et al. 2013, section 5.3 in Ventura et al. 2014). If the majority of the interstellar SiC grains originated from AGB stars are smaller than 0.02 μm or even nanosized, they will be destroyed more rapidly than the currently believed stellar injection rate since the SiC destruction rate increases as the SiC dust size decreases, $(\mathrm{d}M/\mathrm{d}t)_{\mathrm{SiC}}^{\mathrm{des}} \propto 1/a$. In the diffuse ISM, nanosized SiC grains will be stochastically heated by single, individual stellar photons (Draine & Li 2001) and will emit at the Si–C stretch, presumably at 11.3 μm, which, because of the quantum-confinement effect, is expected to differ from the 11.3 μm absorption feature associated with the (crystalline) bulk phase of SiC. Like crystalline silicate nanoparticles, the 11.3 μm emission feature of SiC nanoparticles will probably be hidden by that of polycyclic aromatic hydrocarbon molecules (see Li & Draine 2001).

Admittedly, the average mass-loss rates and total numbers for carbon stars in the Galaxy are not accurately known (see van Loon et al. 2005). The dust production rates of carbon stars depend on the star formation history and metallicity of the galaxy under consideration. The SiC mass fraction depends on the metallicity as well. Nanni et al. (2019) found that the SiC mass fraction could be up to 43 per cent of the total dust mass produced by the carbon stars in the Large Magellanic Cloud and 11 per cent for the Small Magellanic Cloud. However, these are upper limits reached by the dustiest carbon stars, and the spreads in the SiC mass fractions are large (see fig. 9 of Nanni et al. 2019). As a consequence, the injection rate of SiC dust into the ISM may be much smaller. In Groenewegen et al. (1998), where the spectral energy distribution fitting had been performed for carbon stars in the Galaxy, the SiC mass fractions are smaller than 10 per cent for most (37/44) of their stars. Therefore, the non-detection of the 11.3 μm absorption feature of SiC dust could merely be due to a lower injection rate of carbon dust and/or a lower SiC mass fraction than that adopted here.

Alternatively, as argued by Draine (1990), interstellar dust is *not* stardust, i.e. the bulk of the solid material in interstellar grains actually condensed in the ISM rather than in stellar outflows. While carbon stars do eject an appreciable amount of SiC dust into the ISM, supernova shock waves destroy SiC dust (as well as silicate and carbon dust) at a rate faster than its production (McKee 1989), while grain re-growth in the oxygen-rich ISM unlikely leads to SiC.

Finally, we note that the B3LYP hybrid functional employed here had been shown to outperform for SiC cluster systems (see Byrd et al. 2016). While the triangle isomer of Si_3C_3 and the spherical isomer of $Si_{12}C_{12}$ adopted here correspond to their respective global minimum based on DFT calculations made at the M11/cc-pvTZ level of theory (Gobrecht et al. 2017), a different global minimum that is lower than the spherical isomer by > 0.4 eV was found for $Si_{12}C_{12}$ from calculations at the B3LYP/6-311++G(2d,p) level (Byrd et al. 2016). In view of this inaccuracy,

meteorite with a resolution of ~ 50 nm revealed that submicron-sized grains are much more abundant than their larger, micron-sized counterparts (see Hoppe et al. 2010).

Downloaded from https://academic.oup.com/mnras/article/509/4/5231/6415899 by University of Missouri-Columbia user on 13 December 2021

we have also calculated the binding energies for the $O + Si_3C_3$ and $O + Si_{12}C_{12}$ systems using the M11/cc-pvTZ level of theory applied by Byrd et al. (2016). It is found that the energy difference between M11/cc-pvTZ and B3LYP/6-311++G(2d,p) is at most 0.24 eV for $O + Si_3C_3$ and only $\sim$0.01 eV for $O + Si_{12}C_{12}$. Such energy differences will not affect the major results of this work.

5 CONCLUSION

We have utilized molecular dynamics simulations and performed DFT calculations to investigate the oxidation of SiC dust in the ISM. It is found that, although the reaction of an oxygen atom with a SiC molecule is exothermic and could cause CO-loss, the destruction rate of SiC dust through oxidation is considerably smaller than the currently believed stellar injection rate and therefore the non-detection of the 11.3 μm absorption feature of SiC dust in the diffuse ISM cannot be explained by the destruction of SiC dust through oxidation, unless the currently believed SiC dust injection rate from carbon stars is overestimated and/or interstellar SiC dust is considerably smaller than submicron in size.

ACKNOWLEDGEMENTS

The calculations were performed on resources provided by the Swedish National Infrastructure for Computing (SNIC). We thank B.T. Draine, D. Gobrecht, M.A.T. Groenewegen, P.F. Miceli, A. Nanni, D.J. Singh, X.J. Yang, and the anonymous referees for very helpful suggestions. CYX is supported in part by the Talents Recruiting Program of Beijing Normal University and the NSFC Grant No. 91952111. AL is supported in part by NSF AST-1816411 and NASA 80NSSC19K0572.

DATA AVAILABILITY

The data underlying this paper will be shared on reasonable request to the corresponding authors.

REFERENCES

Amari S., Lewis R. S., Anders E., 1994, Geochim. Cosmochim. Acta, 58, 459
Becke A. D., 1992, J. Chem. Phys., 96, 2155
Bernatowicz T., Fraundorf G., Ming T., Anders E., Wopenka B., Zinner E., Fraundorf P., 1987, Nature, 330, 728
Byrd J. N. et al., 2016, J. Chem. Phys., 145, 024312
Chiar J. E., Tielens A. G. G. M., 2006, ApJ, 637, 774
Cristallo S., Nanni A., Cescutti G., Minchev I., Liu N., Vescovi D., Gobrecht D., Piersanti L., 2020, A&A, 644, A8
Dorfi E., Höfner S., 1991, A&A, 248, 105
Draine B. T., 1979, ApJ, 230, 106
Draine B. T., 1990, in Blitz L., ed., ASP Conf. Ser. Vol. 12, The Evolution of the Interstellar Medium. Astron. Soc. Pac., San Francisco, p. 193
Draine B. T., 2011, Physics of the Interstellar and Intergalactic Medium. Princeton Univ. Press, Princeton, NJ
Draine B. T., Li A., 2001, ApJ, 551, 807
Ervin G., 1958, J. Am. Ceram. Soc., 41, 347
Friedemann C., 1969, Astron. Nachr., 291, 177
Frisch M. J. et al., 2016, Gaussian 16, Revision C. 01. Gaussian, Inc., Wallingford, CT
Gehrz R. D., 1989, in Allamandola L. J., Tielens A. G. G. M., eds, Proc. IAU Symp. 135, Interstellar Dust. Kluwer, Dordrecht, p. 445
Gilman R. C., 1969, ApJ, 155, L185
Gobrecht D., Cristallo S., Piersanti L., Bromley S. T., 2017, ApJ, 840, 117
Grimme S., Ehrlich S., Goerigk L., 2011, J. Comput. Chem., 32, 1456
Groenewegen M. A. T., Whitelock P. A., Smith C. H., Kerschbaum F., 1998, MNRAS, 293, 18
Groenewegen M. A. T., Sloan G. C., Soszyński I., Petersen E. A., 2009, A&A, 506, 1277
Helgaker T., Uggerud E., Jensen H. J. A., 1990, Chem. Phys. Lett., 173, 145
Hoppe P., Leitner J., Gröner E., Marhas K. K., Meyer B. S., Amari S., 2010, ApJ, 719, 1370
Kraemer K. E., Sloan G. C., Keller L. D., McDonald I., Zijlstra A. A., Groenewegen M. A. T., 2019, ApJ, 887, 82
Larsson B. et al., 2007, A&A, 466, 999
Lee C., Yang W., Parr R. G., 1988, Phys. Rev. B, 37, 785
Li A., Draine B. T., 2001, ApJ, 550, L213
McKee C. F., 1989, in Allamandola L. J., Tielens A. G. G. M., eds, Proc. IAU Symp. 135, Interstellar Dust. Kluwer, Dordrecht, p. 431
Meyer D. M., Jura M., Cardelli J. A., 1998, ApJ, 493, 222
Min M., Waters L. B. F. M. de Koter A., Hovenier J.-W., Keller L. P., Markwick-Kemper F., 2007, A&A, 462, 667
Mühlhäuser M., Froudakis G., Zdetsis A., Peyerimhoff S. D., 1993, Chem. Phys. Lett., 204, 617
Mutschke H., Andersen A. C., Clément D., Henning Th., Peiter G., 1999, A&A, 345, 187
Nanni A., Bressan A., Marigo P., Girardi L., 2013, MNRAS, 434, 2390
Nanni A., Bressan A., Marigo P., Girardi L., 2014, MNRAS, 438, 2328
Nanni A., Groenewegen M. A. T., Aringer B., Rubele S., Bressan A., van Loon J. T., Goldman S. R., Boyer M. L., 2019, MNRAS, 487, 502
Nanni A., Cristallo S., van Loon J. T., Groenewegen M. A. T., 2021, Universe, 7, 233
Park D. J., Jung Y. I., Kim H. G., Park J. Y., Koo Y. H., 2014, Corros. Sci., 88, 416
Sloan G. C. et al., 2016, ApJ, 826, 44
Speck A. K., Barlow M. J., Skinner C. J., 1997, MNRAS, 288, 431
Treffers R., Cohen M., 1974, ApJ, 188, 545
Uggerud E., Helgaker T., 1992, J. Am. Chem. Soc., 114, 4265
van Loon J. T., Cioni M.-R., Zijlstra A. A., Loup C., 2005, A&A, 438, 273
Ventura P. et al., 2012, MNRAS, 424, 2345
Ventura P., Dell'Agli F., Schneider R., Di Criscienzo M., Rossi C., La Franca F., Gallerani S., Valiante R., 2014, MNRAS, 439, 977
Ventura P., Karakas A., Dell'Agli F., García-Hernández D. A., Guzman-Ramirez L., 2018, MNRAS, 475, 2282
Watkins M. B., Shevlin S. A., Sokol A. A., Slater B., Catlow C. R. A., Woodley S. M., 2009, Phys. Chem. Chem. Phys., 11, 3186
Whittet D. C. B., Duley W. W., Martin P. G., 1990, MNRAS, 244, 427
Wildt R., 1933, Z. Astrophys., 6, 345
Zhukovska S., Henning Th., 2013, A&A, 555, A99

This paper has been typeset from a TEX/LATEX file prepared by the author.

Downloaded from https://academic.oup.com/mnras/article/509/4/5231/6415899 by University of Missouri-Columbia user on 13 December 2021